



Adsorptive potential of coconut fruit shell biochar as low-cost adsorbent for sequestration of rhodamine B dye: kinetics, thermodynamics and phytotoxicity studies

Riti Thapar Kapoor¹ · Mohd Rafatullah^{2,3} · Masoom Raza Siddiqui⁴ · Mahboob Alam⁵

Received: 11 January 2024 / Revised: 22 April 2024 / Accepted: 24 April 2024
© The Author(s), under exclusive licence to Springer-Verlag GmbH Germany, part of Springer Nature 2024

Abstract

The present study aims to use coconut fruit shell biochar (CFSB), an efficient sorbent for Rhodamine B dye (RhB) elimination from aqueous solution. The availability of functional groups and morphology of CFSB surface were analyzed by applying Fourier transform infrared spectroscopy (FTIR) and scanning electron microscopy (SEM). Batch experiments were executed to test impact of pH, contact time, concentration of dye, biochar amount, agitation speed, temperature on RhB dye elimination from aqueous solution by CFSB. Maximum 96% RhB dye removal was reported at pH 2 by CFSB with RhB dye (250 mg/L concentration). Experimental results were found with best agreement with pseudo second order kinetic model. Equilibrium data were explained with Langmuir, Freundlich and Temkin models but results demonstrated best fit with Langmuir model with a higher correlation coefficient ($R^2=0.9818$) and 8.1 mg/g monolayer RhB dye uptake potential. Thermodynamic assessment depicted Gibb's free energy change (ΔG°) had negative values, confirming spontaneity and feasibility of sorption process. Enthalpy (ΔH°) and entropy (ΔS°) changes were 32.039 kJ mol⁻¹ and 92.802 J K⁻¹, respectively. More importantly, even after five adsorption and desorption cycles, CFSB reflected 43% uptake capacity for RhB dye, suggesting that CFSB has a good practical application prospects. Phytotoxicity investigation revealed that CFSB treated solution of RhB dye increased growth of mung bean seedling and biochemical constituents. Therefore, coconut fruit shell biochar can be applied as economic green material for removal of RhB dye from contaminated water and transform industrial effluents into reusable asset.

Keywords Adsorption · Coconut fruit shell biochar · Phytotoxicity · Rhodamine B dye

1 Introduction

The unplanned industrialization, urbanization, rapid population growth, change in climatic conditions and excessive exploitation of natural water resources have raised water safety concerns in recent years [1]. Approximately 70% of the surface of earth is covered by water whereas only < 1% is suitable for consumption purposes [2]. Water pollution has become a serious environmental threat and access to clean water has become a challenging task and an expensive commodity worldwide. According to World Health Organization, around 2.2 billion people are compelled to use contaminated water for drinking and > 800 million people do not have potable water facilities at global level [3]. United Nations sustainable development goals emphasized on the need of availability and sustainable management of water resources by the year 2030 [4]. Dyes are coloured organic pollutants which are used in varied industries like textile,

✉ Riti Thapar Kapoor
rkapoor@amity.edu

¹ Centre for Plant and Environmental Biotechnology, Amity Institute of Biotechnology, Amity University Uttar Pradesh, Noida 201 313, Uttar Pradesh, India

² Environmental Technology Division, School of Industrial Technology, Universiti Sains Malaysia, 11800 Penang, Malaysia

³ Renewable Biomass Transformation Cluster, School of Industrial Technology, Universiti Sains Malaysia, 11800 Penang, Malaysia

⁴ Chemistry Department, College of Science, King Saud University, 11451 Riyadh, Saudi Arabia

⁵ Division of Chemistry and Biotechnology, Dongguk University, 123, Dongdaero, Gyeongju-Si 780714, Republic of Korea

paper, paint, leather, cosmetics and plastics [5]. The textile industries boost economic growth of nation, however these are responsible for more than 20% of global water pollution [6]. More than 800 tonnes of chemical dyes are produced every year from textile industries worldwide and around 10–15% dyes are unable to bind with the fabric and expelled into wastewater during industrial processing [7]. Dye presence in water even at trace concentration reduces water reoxygenation capacity and makes water undesirable for its consumption and application for different purposes [8]. The market for dye stuff was more than thirty billion dollars in 2019 and predicted to cross 49 billion dollars by 2027 [9]. The textile industry utilizes > 230 tonnes water for processing of one tonne of final product [10]. The dye containing effluents released from textile industries are intensively coloured, alkaline, high in biochemical and chemical oxygen demand, total suspended solids and contain salt, detergents, polyvinyl alcohol, surfactants, acids, formaldehyde, oil and heavy metals etc. The presence of noxious dyes in water inhibits light perforation in water, decrease in rate of photosynthesis and shows disastrous impact on aquatic life and entry in human body via food chain [11]. Hence, immediate attention is needed for dye elimination from aqueous system and maintenance of clean environment to safeguard aquatic life, environment and human health.

Rhodamine B, is xanthene basic dye which is amphoteric in nature [12]. It is utilized for manufacturing of ball pens, paints, carbon sheets, crackers, explosives, stamp pad ink, laser dye and textile industry because of its optical properties [13]. It is also utilized as water tracer, photosensitizers, fluorescent markers for analysis of microscopic structures and biological stain in biomedical research [14]. Rhodamine B dye is soluble in water and presence of very low concentration of RhB (1 ppm), imparts intensive colour to water and makes it unfit for consumption and domestic applications [15]. Rhodamine B has high photostability, non-biodegradable nature and presence of N-ethyl groups on xanthene rings makes it toxic [16]. Exposure of RhB dye to algae, crustaceans and fishes reflected lethal concentration (LC50 which shows 50% mortality) in the range from 14 to 24 mg/L. The annual average quality standard and maximum allowable concentration quality standard for RhB dye were found to be 14 and 140 µg/L, respectively. Thus, concentration below 140 µg/L for RhB dye is not expected to pose a risk on aquatic life as observed during tracer experiments [17]. Rhodamine B causes allergic dermatitis, irritation and redness of skin, eyes, disruption of central nervous system, gastrointestinal and respiratory tracts and damage to kidney, liver and thyroid gland [15]. International Agency for Research on Cancer classified Rh B as a Group 3 carcinogen [18]. The photosynthetic and antioxidant activities of *Hydrilla*

verticillata were adversely affected by RhB dye exposure [19]. *Chlorella vulgaris* exposure to RhB dye (50 mg/L) for 96 h significantly reduced pigment and protein components [20]. Kooh et al. [21] observed hazardous effects of RhB dye on *Cyprinodon variegatus* at 84 mg/L concentration. Different animal models reflected liver enlargement and weight loss after oral intake of 1% RhB dye in feed up to three months [22]. They also reported death of rats within two minutes after intravenous administration of lethal dose of RhB dye (90 mg/kg). Sulistina et al. [23] reported RhB dye enhanced apoptosis of brain cells and disrupted balance of hormones in mice.

Different procedures have been used for elimination of dye from aqueous system like photocatalysis, flocculation, ozonation, coagulation, electrolysis, advanced oxidation, and membrane technology etc. [24]. Many commercial adsorbents like activated carbon, clay, zeolite, polymer and metal–organic frameworks have been explored for wastewater treatment [25]. However, various drawbacks are associated with the above-mentioned technologies such as high cost, energy consumption, less efficiency, complex and labour-intensive procedure, requirement of large treatment area and sludge generation. Adsorption has been endorsed as an effective, affordable, sustainable, reliable and widely accepted method for elimination of colouring materials from contaminated water because of more efficacy and suitable for large scale applications [26]. Agricultural sector produces > 1300 million tonnes of biomass waste every year, burning and disposal of agro-wastes generate greenhouse gases, air, water and soil pollution and depletion of microbial population in soil which poses serious problems for environment and health of human-beings [27]. Lignocellulose rich agricultural wastes have been regarded as one of the best alternatives for elimination of dye because of easy accessibility, low-cost, more uptake efficiency, simple design, easy operation and reusability which can be important attributes for development of circular bio-economy [28, 29]. Therefore, conversion of agro-wastes into biochar as valuable adsorbent for dye removal from aqueous system will be a promising option due to availability of wide range of raw materials, simple preparation process, low cost, remarkable adsorption capacity and feasibility [30]. Biochar, carbon rich porous material produced from biomass pyrolysis without oxygen has shown large specific surface area, porosity, enriched surface binding sites, cation exchange ability, renewability and stability convert into superior sorbent for pollutants elimination from wastewater [31]. Different crop residues and biomass wastes such as wheat straw, rice and peanut husks, fruit and vegetable peel, tea waste, microalgae and sewage sludge have been used for preparation of biochar [32]. The agricultural wastes

utilization enhances recycling of wastes which are available at zero cost and promotes circular economy and carbon neutrality towards sustainable environment [33]. *Vigna radiata* L. (Family: Fabaceae), commonly known as mung bean or green gram, is important legume crop which is cultivated in different parts of globe in around six million hectare area [34]. Mung bean, also considered as poor man's meat, is excellent source of proteins, antioxidants, minerals, vitamins and essential fatty acids [35]. The coconut (*Cocos nucifera* L.; family: Palmae) is an economically important crop, known as tree of life and cultivated in ~ twelve million hectares of tropical and sub-tropical parts of the world. To the best of our information, no report is available on the effect of coconut fruit shell biochar for RhB dye adsorption and impact of CFSB treated RhB dye solution on growth and biochemical variables of *Vigna radiata*. Present investigation was designed to analyze characterization of coconut fruit shell biochar, sorption performance of CFSB for RhB dye which was systematically investigated with adsorption isotherm, kinetics, thermodynamic variables and reusability of CFSB treated wastewater was tested on development and biochemical variables of mung bean plants.

2 Materials and methods

2.1 Biochar preparation

Coconut fruit shells were collected from fruit vendor from local market of Noida. The coconut fruit shells were cleansed properly with tap water, then with distilled water for elimination of dust particles. Coconut fruit shells were kept under sunlight for fifteen days until they become hard by reducing moisture content, then broken into small pieces with stainless-steel electronic grinding machine. A stainless-steel pyrolysis reactor (length: 1.1 m and inside diameter: 75 mm) was used for biochar production from coconut fruit shell with temperature controlled by an electric heater. Nitrogen was purged in pyrolyzer for 60 min at the rate of $100 \text{ cm}^3 \text{ min}^{-1}$ to maintain the inert atmosphere. The crushed coconut fruit shells were pyrolyzed at $500 \text{ }^\circ\text{C}$ (heating rate: $10 \text{ }^\circ\text{C min}^{-1}$) for 4 h.

Prepared biochar was cleansed with autoclaved deionized water and placed for two hours in oven at $65 \text{ }^\circ\text{C}$ to check activities of microbes [36]. The effect of different biochar particle sizes on the RhB dye adsorption process was also analyzed. After the preparation of CFSB, we standardized biochar particle size by sieving process with using different sieves such as 80 BSS mesh (0–170 μm), 72 BSS mesh (230–300 μm) and 45 BSS mesh (320–500 μm).

2.2 Proximate analysis of CFSB

Proximate analysis of CFSB was carried out to assess stability of biochar towards thermochemical process. Coconut fruit shell biochar (2 g) was kept in a crucible at $110 \text{ }^\circ\text{C}$ in hot air oven for 60 min for calculation of moisture content. For volatile content, CFSB (2 g) was taken in a closed crucible and placed at $900 \text{ }^\circ\text{C}$ for 10 min in a muffle furnace whereas for ash content, CFSB (2 g) was kept in open crucible at $775 \text{ }^\circ\text{C}$ for 60 min in muffle furnace [37]. Fixed carbon content was calculated by the following Eq. 1:

$$FC (\text{wt}\%) = [100 - VM + AC + MC] \quad (1)$$

where, FC = fixed carbon, VM = volatile matter, AC and MC are ash and moisture contents, respectively.

2.3 Preparation of reagents

Rhodamine B dye was procured from Sigma-Aldrich, Bangalore, India. Seeds of mung bean (*Vigna radiata* L. variety Virat) were procured from seed agency of Noida. RhB dye stock solution (1000 mg L^{-1}) was prepared and diluted to different concentrations with distilled water. UV–vis spectrophotometer (Shimadzu 1800) was used for measuring dye solution optical density. Reagents applied for experiments were of analytical grade. RhB dye properties are mentioned in Table 1.

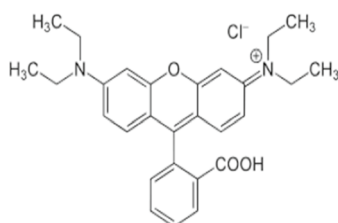
2.4 Batch study

Batch investigation was executed to assess CFSB viability as sorbent for RhB dye removal from aqueous medium. Impact of different experimental parameters like pH (2–10), size of particles (0–500 μm), contact period (20–120 min), biochar dose (1–3.5 g), concentration of dye (100–350 mg/l), agitation speed (50–300 rpm), and temperature ($30\text{--}55 \text{ }^\circ\text{C}$) were utilized for RhB dye elimination from aqueous medium with CFSB. RhB dye solution (100 ml) of different (100, 150, 200, 250, 300 and 350 mg/l) concentrations were taken in six distinct flasks, CFSB amount 1, 1.5, 2, 2.5, 3 and 3.5 g were mixed, respectively. In control, CFSB was not mixed in RhB dye solution. Absorbance was measured by UV–vis spectrophotometer ($\lambda_{\text{max}} = 554 \text{ nm}$), The RhB dye removal percentage (%) and adsorption capacity were calculated by given Eqs. (2) and (3):

$$\text{RhB dye removal (\%)} = (C_o - C_t) / C_o \times 100 \quad (2)$$

Table 1 Properties of Rhodamine B dye

Dye Stuff	Basic Violet 10, Brilliant Pink B, Basic Rose Red
C.I. Number	45170
Color	Red violet coloured powder
Type	Cationic dye
Melting point	210–211°C
Solubility	Soluble in water and organic solvents
IUPAC name	N-[9-(ortho-carboxyphenyl)-6-(diethylamino)-3H-xanthen-3-ylidene] diethyl ammonium chloride
Formula	C ₂₈ H ₃₁ N ₂ O ₃ Cl
Molecular weight	479 g/mol
Application	Textile, paper and printing industries
Structure	



λ_{\max} 554 nm

C_0 and C_t = Initial and final concentrations of RhB (mg/l).

$$q_t = \frac{(C_0 - C_t)}{m} * V \quad (3)$$

whereas, C_0 is initial concentration of RhB dye (mg L^{-1}), C_t is equilibrium concentration of RhB dye (mg L^{-1}), V is volume of solution (L), and m is mass of adsorbent (g).

2.5 Point of zero charge

Point of zero charge was analyzed by method of Rivera-Utrilla et al. [38]. The 0.10 M HCl and NaOH solution were used to maintain 0.01 M NaCl solution range from pH 3–11. One gram CFSB was added in different solution, placed for one day at room temperature, pH_{final} was analyzed. pH_{PZC} was assessed by graphical plot by using formula: $\text{pH}_{\text{final}} - \text{pH}_{\text{initial}} = f(\text{pH}_{\text{initial}})$.

2.6 Coconut fruit shell biochar characterization

The surface characteristics of CFSB were described based on the presence of active available functional groups. Potassium bromide (KBr) pellet method was used for

detection of binding sites available on CFSB before and after adsorption of RhB dye by FTIR spectra (Perkin Elmer 2000, Waltham, MA, USA). The active sites on the adsorbent surface were obtained from FTIR spectrum and recorded by using the transmittance mode conducted over wavelengths of 500 and 4000 cm^{-1} after mixing adsorbent sample thoroughly with KBr in a mortar and then put into a pellet-forming die. The peaks were obtained in less than 30 s of scanning time.

The surface morphology of CFSB was depicted with SEM (Quanta FEG 650, Thermofisher, Beverly, CA, USA). The morphology of CFSB before and after RhB dye adsorption was obtained from scanning electron micrographs. The sample was prepared on aluminum plate. Prior to analysis, samples were wrapped with gold foil using a sputter coater (SCD050) to improve the conductivity. The morphology of the CFSB was captured at an accelerating voltage of 15 kV.

2.7 Kinetics of dye uptake process

Kinetic investigation is needed for analysis of order of reaction in adsorption system and to identify controlling process for sorption mechanism. Pseudo first (PFO), Pseudo second order (PSO), Weber-Morris intraparticle diffusion (WMIPD) models were applied for determination of rate constant for sorption process.

Pseudo first order model was explained by Lagergren [39], which defines sorption process was related to diffusion and physisorption. This model deals with single sorption site for single dye molecule and sorption with time corresponded to instant efficacy [40]. Variables can be achieved by plotting logarithmic parameters ($\ln(q_e - q_t)$) with time as given in Eq. 4:

$$\ln(q_e - q_t) = \ln q_e - k_1 t \quad (4)$$

q_e = RhB dye uptake at equilibrium, q_t RhB dye uptake at time, and k_1 = pseudo first order uptake rate constant (min^{-1}).

The sorption of single dye molecule onto two active sites of sorbent can be described by pseudo second order model (Eq. 5) [41], in which sorption process is regulated with chemisorption process, which includes valency forces via transmission between CFSB and RhB dye and electron sharing [42].

$$t/q_t = 1/k_2 q_e^2 + t/q_e \quad (5)$$

q_e = RhB uptake on CFSB at equilibrium, k_2 = pseudo second order sorption rate constant (g/mg.min).

Kinetic results were also analyzed by applying WMIPD model (Eq. 6) proposed by Webber and Morris [43]. It explains mechanism of diffusion and dye molecules transfer via the internal pores. Dye sorption is proportional to $t^{1/2}$ as compared to t . Initial rate constant (k_{diff}) and thickness of boundary layer (C) was obtained by plotting qt vs. $t^{1/2}$. All these values are required for identification of sorption process and prediction of rate regulating step.

$$q_t = k_{diff}t^{1/2} + C \quad (6)$$

k_{diff} = intraparticle diffusion rate constant ($\text{mg/gmin}^{0.5}$), q_t = sorption ability in t (mg g^{-1}), C = boundary layer thickness.

2.8 Adsorption isotherm

Various isotherm models were applied for estimation of equilibrium sorption. RhB dye (250 mg/l) was mixed with different doses of CFSB for isotherm viability assessment through analyses of their potential for dye uptake.

2.8.1 Langmuir isotherm

The Langmuir model is based on the assumption that adsorption takes place in monolayer form without any interaction between adsorbed molecules. Based on this model, adsorption energies onto.

the CFSB surface are uniform [44]. It can be written as mentioned in Eq. 7:

$$\frac{C_e}{q_e} = \frac{1}{q_m K_L} + \frac{C_e}{q_m} \quad (7)$$

q_e = RhB sorption at equilibrium (mg g^{-1}), q_m = maximum RhB adsorption (mg g^{-1}), C_e = RhB concentration at equilibrium (mg L^{-1}), K_L = Langmuir constant related with binding of RhB dye on CFSB.

2.8.2 Freundlich isotherm

It deals with RhB dye dissipation between solution and CFSB at equilibrium. This shows difference in binding sites energy enhancement for adsorption and reduction in adsorption heat [45]. It can be denoted as following (Eq. 8):

$$\ln q_e = \ln K_F + \left(\frac{1}{n}\right) \ln C_e \quad (8)$$

K_F = sorption ability, n = intensity.

Dye uptake can be explained as chemisorption when $n < 1$, physisorption at $n > 1$, linear sorption when $n = 1$.

2.8.3 Temkin isotherm

Temkin isotherm explains that adsorption heat of RhB dye molecules in a layer reduces with coverage due to interaction between dye and CFSB and adsorption shows consistent dispersal of binding energies to their highest level. The model assumed that adsorption energy reduced due to the interaction between CFSB surface and RhB dye. Temkin isotherm is given below as Eq. 9 [46].

$$q_e = R_T/b_T \ln(A_T) + RT/b_T \ln(C_e) \quad (9)$$

A_T = Temkin isotherm constant (l g^{-1}), b_T = Temkin constant for adsorption heat (J mol^{-1}), R = gas constant (J/mol.K), T = absolute temperature.

2.9 Thermodynamic parameters

The alteration in ΔG , ΔH , ΔS were determined for RhB dye adsorption by CFSB. Thermodynamic parameters were analyzed with given in Eqs. 10, 11 and 12:

$$\Delta G^0 = -RT \ln K_d \quad (10)$$

$$K_d = \frac{q_e}{C_e} \quad (11)$$

$$\Delta G^0 = \Delta H^0 - T \Delta S^0 \quad (12)$$

The changes in ΔG , ΔH , ΔS were studied after the rearrangement of equation and with the use of a curve fitting procedure for adsorption mechanism.

Where ΔG = Gibbs free energy (kJmol^{-1}), K_c (L g^{-1}) = equilibrium partition constant, T ($^{\circ}\text{C}$) = temperature, R = universal gas constant ($8.314 \text{ Jmol}^{-1} \text{ K}^{-1}$), ΔH (kJ mol^{-1}) and ΔS (JK^{-1}) were standard enthalpy and entropy changes, respectively.

2.10 Assessment of reutilization capacity

Coconut fruit shell biochar (2 g) was mixed in RhB dye (250 mg/l concentration), kept in shaking incubator at 200 rpm for 80 min at 28 ± 2 $^{\circ}\text{C}$. After centrifugation, CFSB containing RhB dye was separated, and absorbance of the supernatant was measured to analyze the uptake of RhB dye by CFSB. CFSB with RhB dye was kept at 50°C for 6 h for enhancement in CFSB microstructures and dye sorption efficiency. Coconut fruit shell biochar was cleansed with 1N HCl and NaOH, kept for 45 min at 180 rpm, then desorbing solution absorbance was measured [47]. For removal of desorbing solution, CFSB was separated and rinsed properly with autoclaved deionized water and CFSB was placed at

50 °C for eight hours. Efficiency of CFSB was tested by five successive cycles. RhB desorption percentage was estimated with given Eq. 13:

$$\text{Desorption (\%)} = \text{RhB dye desorbed} / \text{RhB dye adsorbed} * 100 \quad (13)$$

2.11 Phytotoxicity assessment

The phytotoxic impact of Rhodamine B dye before and after CFSB treatment was assessed on mung bean. The seeds were rinsed with distilled water, then their surface were treated with mercuric chloride (0.1%) for 5 min to inhibit microbial infestation, further cleansed with Milli-Q water. Ten seeds of mung bean were kept in three set of test tubes containing distilled water, RhB solution (250 mg/l), solution of RhB dye treated with CFSB, respectively for four h. Then, *Vigna radiata* seeds were kept in sterilized petriplates and kept in seed germinator with 88% relative humidity at 26 ± 2 °C under 12 h light for 2 weeks. ISTA [48] procedure was applied for assessment of seed germination, seedling length, biomass and vigour index (Eqs. 14 and 15).

$$\text{Germination (\%)} = \text{Mung bean seeds germinated} / \text{mung bean seeds taken for germination} * 100 \quad (14)$$

$$\text{Vigour index (VI)} = \text{germination (\%)} \times \text{seedling length} \quad (15)$$

2.12 Analyses of biochemical variables

Chlorophyll content was examined by Lichtenthaler [49]. Sugar and protein components were estimated in mung bean plants by Hedge and Hofreiter [50], Lowry et al. [51] procedures, respectively.

2.13 Statistical analysis

Three replicates were used in randomized block design for each treatment. ANOVA and SPSS were applied for estimation of data. Mean of treatment was assessed by Duncan's multiple range test at $P < 0.05$.

3 Results and discussion

In the present study, biochar prepared from coconut fruit shell (CFSB) was used for removal of RhB dye from aqueous solution. The characterization of prepared CFSB was carried out by proximate analysis, FTIR and SEM and effect of different parameters was evaluated by batch experiments for RhB dye removal by CFSB and effect of CFSB treated

RhB dye solution on the growth of *Vigna radiata* seeds was also evaluated by phytotoxicity assessment.

3.1 Proximate estimation of coconut fruit shell biochar

Proximate analyses were executed to analyse fixed carbon, water content, volatile material, ash in CFSB. Due to heat treatment under pyrolysis, biomass material releases gases and liquid leaving high carbon content material. The high content of fixed carbon reflects better quality of sorbent because of large surface area and increased uptake efficiency. Results revealed more volatile material and fixed carbon, while less moisture as given in Table 2.

3.2 Characterization of CFSB

3.2.1 Morphological properties

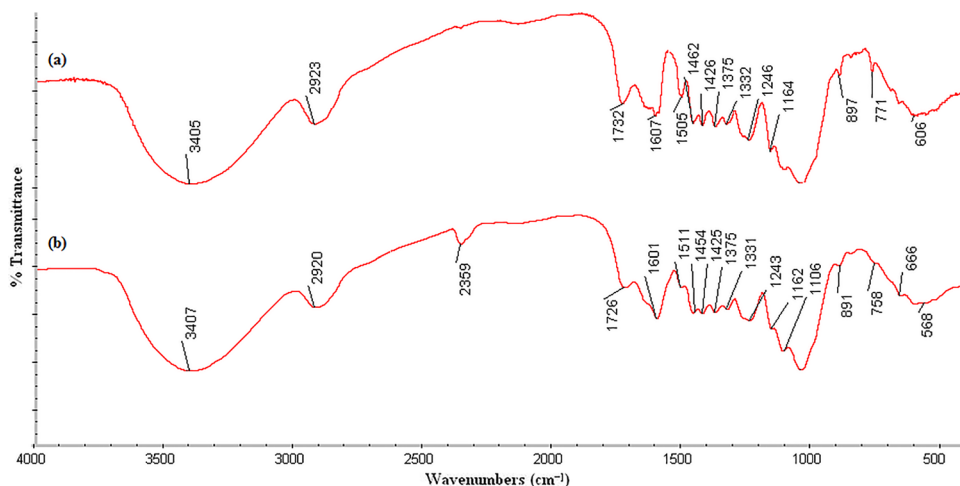
The binding sites available on CFSB surface are important for sorption studies and wastewater treatment process. The structure of sorbent material and adsorption capacity are affected with active sites present on sorbent surface. Pyrolysis temperature and feedstock material determine the availability of functional groups on biochar surface [52].

Figure 1 shows FTIR spectrum of CFSB from wavenumber 500–4000 cm^{-1} . Figure 1(a) shows FTIR of CFSB before adsorption of RhB dye whereas 1(b) reflects FTIR of CFSB after adsorption of RhB dye. The shift in peak and reduction in peak intensities are clearly visible in FTIR spectra in Fig. 1(b) after RhB dye adsorption because of intra and intermolecular interactions between RhB dye and functional groups of CFSB. The FTIR spectrum shows absorption band at 3405 cm^{-1} , corresponding to the hydroxyl group stretch, which is present in lignocellulosic materials and indicates presence of phenolic compounds, alcohol and moisture in CFSB. The adsorption band at 2923 cm^{-1} shows presence of alkyl groups (CH_2 and CH_3) in the structure [53]. At 1732 cm^{-1} , strong carbonyl stretch is present, which indicates CFSB material is rich in carboxylic acids, ketones and esters originated from sugars such as xylene and lignin and from non-polar compounds like fatty acids or their derivatives. The spectrum reflects adsorption band at 1607 cm^{-1} ,

Table 2 Proximate analysis of CFSB

S.No	CFSB	Weight (%)
1	Moisture	09.56
2	Volatile matter	54.75
3	Ash	14.23
4	Fixed carbon	21.46

Fig. 1 FTIR of CFSB (a) before RhB dye adsorption and (b) after RhB dye adsorption



indicating presence of C=C linkages from various sources, including aromatic rings [54]. The stretches at 1246 cm^{-1} and 1164 cm^{-1} , derived from C–O bonds of both Csp^2 and Csp^3 [55]. The adsorption band at 771 cm^{-1} may be due to the presence of alcohol, ketones and aldehydes. In Fig. 1(b) stretch at 568 cm^{-1} indicates the presence of sugars like cellulose and hemicellulose [56, 57]. The presence of C–O group is indicated by the peak appeared at 1106 cm^{-1} . The $\text{Csp}^3\text{-O}$ group comes from ether and polysaccharides, which may be due to stretch of C–O–C at 1106 cm^{-1} [58]. These bands reflect the presence of polar groups in CFSB which may interact through hydrogen bonds and dipole–dipole interactions with compounds that have hydroxyl and amino groups in their structure [53]. The peak at 891 cm^{-1} is due to C–H functional group [59]. When we compared both FTIR spectra i.e. before and after RhB dye adsorption, we noted that some bands at 1505 cm^{-1} , 771 cm^{-1} and 606 cm^{-1} disappeared, and some previously observed bands exhibited their reduced transmittance intensity, suggesting interaction between RhB dye molecules and CFSB or chemisorption mechanism [60].

SEM was done to analyze alterations in surface morphology of CFSB. The details of surface structure are important for sorbent material use in sorption studies as it facilitates understanding of dye uptake phenomenon which takes place on surface of biochar and inside pores. Coconut fruit shell biochar SEM images prior and after adsorption process were analyzed at 5 KX magnification resolution with $2\text{ }\mu\text{m}$ CFSB particle size. The SEM image indicates that CFSB had irregular surface with various pores and this type of morphology facilitates intermolecular and intramolecular interactions between CFSB and RhB dye [61]. Notable modifications were detected in CFSB after RhB dye uptake in comparison to CFSB without RhB. After pyrolysis of coconut fruit shell, volatilization of organic substances shows porous and heterogeneous structure because of changes in CFSB due to lignin oxidation produced carboxyl, hydroxyl, carbonyl groups (Fig. 2a). Tightly bound surface was visible after

RhB dye uptake, as binding sites available on CFSB were occupied with RhB dye molecules after CFSB interaction (Fig. 2b).

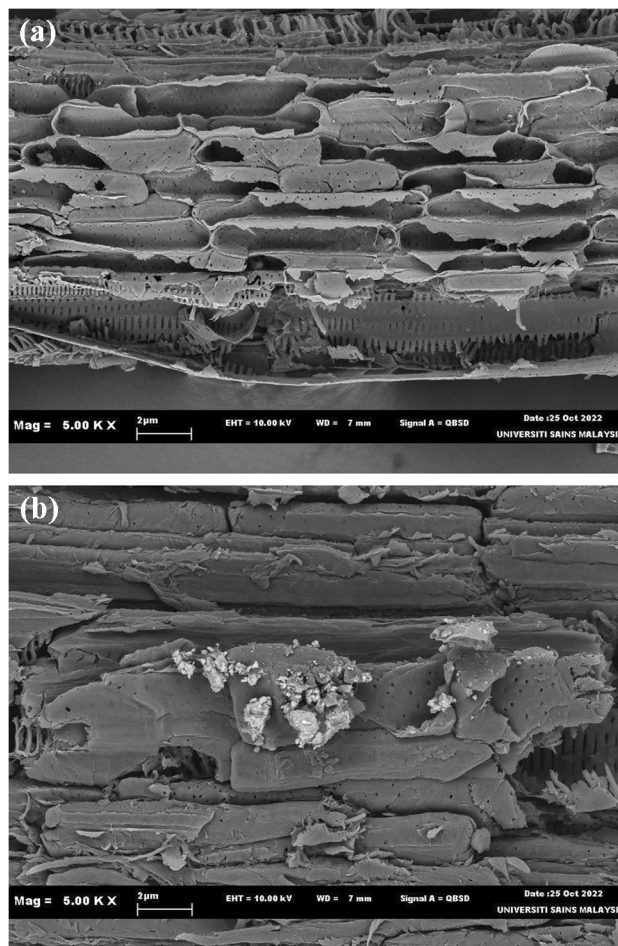


Fig. 2 Scanning electron micrographs of CFSB before and after RhB dye sorption process (a) corresponds to CFSB with pores before RhB dye adsorption, (b) reflects CFSB with filled pores with RhB dye after adsorption

3.3 Batch experiments

Effect of various parameters like pH, particle size, contact period, concentration of dye, biochar dose, agitation speed, temperature were measured for RhB dye elimination from aqueous solution by CFSB (Fig. 3). Sorption efficiency of CFSB and adsorption processes mechanism were analysed by different isotherm and kinetic models and thermodynamics parameters.

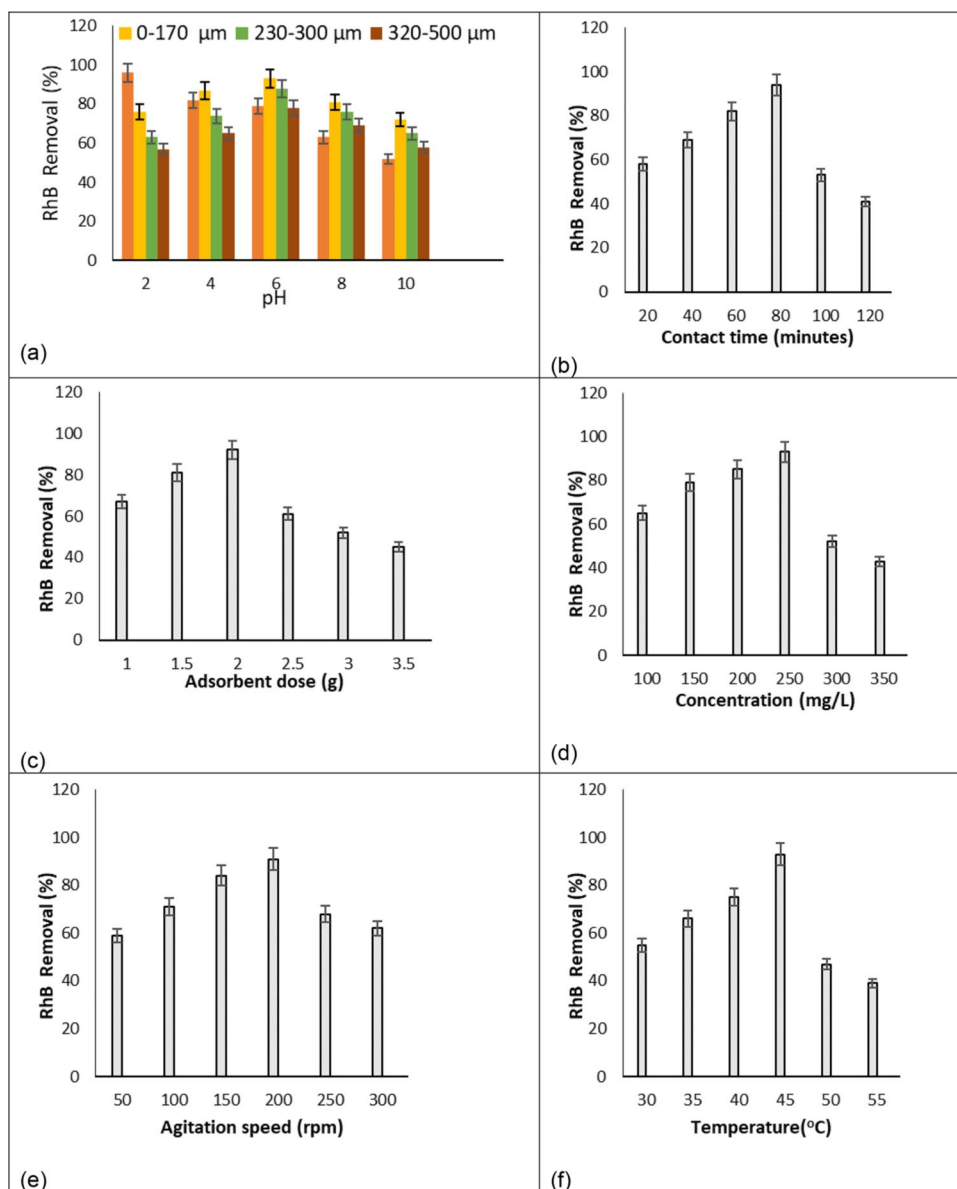
3.3.1 Effect of pH

pH is crucial factor which determines efficiency of sorbents. pH of solution influences dye solubility, physico-chemical properties of biochar surface, dye speciation and

degree of ionization and sequestration of dye onto sorbent surface [62]. Figure 3(a) reflects both effect of pH (2–10) and three different CFSB particle sizes on removal of RhB dye. First bar denotes pH and subsequent 3 bars are presenting three different CFSB particle sizes (0–170 μm , 230–300 μm and 320–500 μm).

In this study, we examined effect of different pH range (2–10) on RhB dye sorption onto CFSB at $26 \pm 2^\circ\text{C}$ (Fig. 1a). Maximum 96% RhB dye sorption was reported at pH 2 and pH 4, 6, 8 and 10 showed 82, 79, 63 and 52% RhB dye elimination, respectively. The possible explanation for this could be at the point of zero charge (pHpzc), both positive and negative electrical charges present at the adsorbent surface are balanced. The effect of pHpzc on adsorption process can be observed in three ways: (i) adsorbent surface shows negative

Fig. 3 Impact of parameters (a) pH, size of particles (b) contact time (c) dye concentration (d) CFSB amount (e) speed of agitation (f) temperature on removal of RhB dye (250 mg/l) with CFSB



charge if $pH_{pzc} < pH$, (ii) adsorbent surface reflects positive charge if $pH_{pzc} > pH$, and (iii) adsorbent surface is neutral if $pH_{pzc} = pH$ [63]. In the present study, pH_{pzc} of CFSB was 5.4, hence at pH 2, the surface of prepared CFSB was positively charged and it attracts the ionic form of RhB dye and led to enhanced adsorption [64]. The FTIR results confirm stretches of carbonyl, hydroxyl, methylene and methyl groups on CFSB, it indicates presence of carboxylic acids, esters, ketones in their structure. Hence, low pH promotes hydrogen bonding of carboxyl and tertiary amine groups of RhB dye molecules and gets protonated to oxygenated groups and show polar behaviour [57]. At high pH, deprotonation of benzoic acid of RhB dye takes place and it promotes change in the charge on RhB dye molecule from positive to negative [65]. Besides, rise in pH tends to dissociate phenolic hydroxyl groups of CFSB, thus, repulsion between CFSB and RhB dye having the same net charges [66]. Ren et al. [67] reported that molecules of RhB dye shows cationic form at less $pH < 3$, and zwitterion form at $pH > 5.0$. Due to deprotonated form of $-COOH$ groups on RhB dye, transformation from cationic to zwitterionic or dimer form may occur which in turn leads to electrostatic repulsion between RhB dye and negatively charged CFSB, thus reducing its adsorption capacity. Mousavi et al. [68] recorded maximum 89% removal of RhB dye at pH 3 by stalk corn activated carbon.

Similar findings were reported by earlier researchers in which reduction in RhB dye sorption was reported with biochar of walnut shells [69] and *Casuarina equisetifolia* needles [21] with rise in pH value. Khan et al. [70] reported 98% RhB removal at pH 3.6, after 27 min by polymeric Dowex. Wu et al. [71] recorded more elimination of RhB dye at pH 4.69.

3.3.2 Size of particle

The size of biochar particles influence heat rate and mass transfer of particles. Three different CFSB particle sizes 0–170, 230–300 and 320–500 μm were utilized to assess particle size effect on RhB dye adsorption. Figure 3(a) reflects both effect of pH (2–10) and three different CFSB particle sizes on removal of RhB dye. First bar indicates pH and subsequent 3 bars are presenting three different CFSB particle sizes (0–170 μm , 230–300 μm and 320–500 μm). With decrease in CFSB particle size, RhB dye uptake enhanced, due to large surface area on small sized particles increased uptake of RhB (Fig. 3a). The diffusion resistance towards mass transmission was higher for big CFSB particles, inner surface could not applied for dye uptake, therefore low sorption of RhB was reported.

3.3.3 Contact time

RhB dye uptake at distinct exposure time and subsequent time to obtain uptake equilibrium is important factor for

uptake [72]. For assessment of contact time, we selected CFSB particle size (0–170 μm), adsorbent dose (1–3.5 g) and pH 2. Elimination of RhB dye (250 mg/l) 58, 69, 82 and 94% was observed at 20, 40, 60 and 80 min, respectively. Driving pressure of concentration gradient between CFSB and RhB dye was more and rate of sorption was high at initial contact period. Uptake of RhB dye was fast during initial 80 min, continuously lowered and finally obtained equilibrium after that dye uptake was significantly reduced (Fig. 3b). As time progressed, RhB dye molecules gradually filled adsorbent active sites, vacant spaces which were available initially, with rise in time RhB dye molecules were entered in spaces and all the sites were filled and uptake of dye become arduous and increasing trend of dye uptake get reduced.

3.3.4 Adsorbent amount

Dose of adsorbent is an important factor for determination of sorption efficacy of adsorbent. To find out the optimal adsorbent dose, impact of various amount of CFSB on RhB dye removal was investigated (Fig. 3c). Rhodamine B dye elimination efficiency was increased rapidly from 67–92% with increasing amount of CFSB from 1–2 g. It was because of binding sites availability which facilitate dye adsorption process. The adsorbent dose affects dye and biochar equilibrium in sorption process. Maximum 92% RhB dye removal was reported with 2 g CFSB. With rise in biochar dose, surface area and availability of binding sites enhances dye uptake capacity of CFSB. However, rise in amount of CFSB above optimum level, RhB dye elimination efficiency did not reflect any notable changes. It was because of CFSB particles compacted together or cluster formation by molecules of dye or overlap of sorption spaces which cover the pores and vacant sites were not available for dye uptake hence decreased dye elimination efficacy [73]. Decolorization of RhB dye solution was enhanced from 37–84%, when animal bone meal adsorbent dose was enhanced from 10 to 90 mg [74].

3.3.5 Dye concentration

Initial dye concentration plays pivotal function for effective adsorption process. Rise in dye concentration in solution enhances mass gradient between RhB dye solution and CFSB, acts as a driving force for dye molecules movement towards CFSB surface from solution [75]. Concentration gradient force could not push RhB molecules to drag via transfer resistance between RhB and CFSB at low concentration of dye, unoccupied spaces were accessible for dye uptake on CFSB, these results were retracted with rise in concentration of dye.

Elimination of RhB dye was enhanced with increase in concentration of RhB dye, but with high amount of RhB

dye, rate of dye uptake was decreased (Fig. 3d). Maximum 93% RhB dye sorption was reported with 250 mg/L dye. Dye uptake was decreased, if RhB dye concentration further raised, reflected that sorption rate was restricted with high concentration of RhB dye. The RhB dye sorption was enhanced significantly at initial step, which was because of accessibility of unoccupied functional groups on CFSB surface [35]. Sorbent has fixed number of functional groups which saturate at certain concentration, and RhB dye in solution do not attach to active spaces on CFSB or RhB dye aggregation onto solid phase [76]. Reduction in dye uptake capacity with increase in RhB dye concentration might be because of competition between dye ions for unoccupied spaces available for dye uptake. Saigl and Ahmed [77] reported by enhancing concentration of dye from 0.5 to 80 mg/l, RhB dye elimination efficacy was reduced from 98 to 30%.

3.3.6 Speed of agitation

RhB dye removal was increased with rise in speed of agitation (50–300 rpm) as observed in Fig. 3e. The increase in agitation speed decreases boundary layer obstruction for RhB dye transfer to CFSB from solution [78]. With rise in agitation speed, interaction between RhB dye molecule and CFSB particles were enhanced because of rise in dispersion degree of CFSB in solution of dye. High agitation speed requires high energy and significant rise in RhB dye removal was not recorded at 250 and 300 rpm and 200 rpm agitation speed was optimum speed which reflected 91% RhB dye uptake.

3.3.7 Temperature

Rhodamine B dye uptake on CFSB was reported at different temperature such as 30, 35, 40, 45, 50 and 55 °C. Rhodamine B dye exhibited 55, 66, and 75% sorption at 30, 35, 40 °C respectively, highest 93% RhB dye removal was recorded at 45 °C (Fig. 3f). Enhanced RhB dye elimination was reported at high temperature because of increase in mobility of RhB molecules by rise in temperature and binding sites availability. With increase in reaction temperature, biochar surface area increases due to reduction in oxygen-containing functional groups from its surface [79]. However, RhB dye uptake was reduced at 50 and 55°C, which indicated sorption procedure was controlled by heat generation. This might be attributed to higher kinetic energy of RhB dye molecules when the temperature increases, which can reduce the electrostatic attraction and separate RhB dye molecules from CFSB surface. Hence, very high temperature will not force the RhB dye molecules to diffuse inside the pores of CFSB. Similar findings were observed by earlier researchers. The adsorption of congo red dye onto burned

root of *Eichhornia crassipes* reflected that physical bonding between the dye molecules and active sites of *Eichhornia crassipes* weaken by increasing temperature [80]. Hu et al. [81] recorded adsorption of congo red from aqueous solution by cattail root reduces with increase in temperature.

3.3.8 Point of zero charge

The point of zero charge (pHpzc) plays pivotal role in the surface characterization of adsorbent. At point of zero charge (pHpzc), both positive and negative electrical charges present onto CFSB surface are balanced. If $\text{pHpzc} < \text{pH}$, CFSB surface shows negative charge, if $\text{pHpzc} > \text{pH}$, adsorbent surface reflects positive charge and retention of negatively charged species is favoured and adsorbent surface is neutral if $\text{pHpzc} = \text{pH}$ [63]. In the present study, pHpzc of CFSB was 5.4 (Fig. 4), hence at pH 2, the surface of prepared CFSB was positively charged and it attracts the ionic form of RhB dye and led to enhanced adsorption [64]. The deprotonation of carboxylic acid groups on RhB dye, assists transformation of its cationic to zwitterionic form which may lead to electrostatic repulsion between RhB dye and negatively charged CFSB, thus reducing its adsorption efficacy.

3.3.9 Adsorption kinetics

Kinetic investigation was applied to assess sorption rate of RhB dye by CFSB and sorption process mechanism. Sorption kinetics explains how resistance to mass transfer takes place between CFSB and RhB dye molecules. Three models such as PFO, PSO and WMID were used to predict sorption kinetics involved in RhB dye adsorption and possible rate-controlling steps through fitting experimental results. Fast sorption of RhB dye was reported at the beginning of experiment, which was significantly reduced after 80 min due to saturation of available vacant sites onto biochar [29]. The pseudo-first order equation is based on

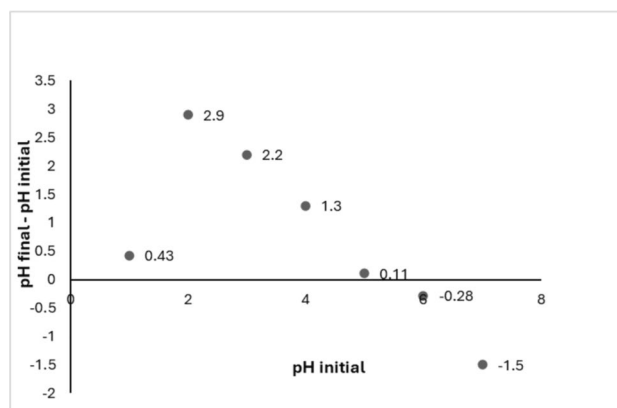


Fig. 4 A graphical plot of the point of zero charge of CFSB

Table 3 Kinetic model application for sorption of RhB dye on CFSB

Model	Equation	Variables	Value
PFO	$\ln(q_e - q_t) = \ln q_e - k_1 t$	k_1 (min^{-1})	0.0282
		q_e (mg g^{-1})	16.3267
		R^2	0.6888
PSO	$\frac{t}{q_t} = \frac{1}{k_2 q_e} + \frac{t}{q_e}$	K_2 ($\text{g mg}^{-1} \text{min}^{-1}$)	0.00489
		q_e (mg g^{-1})	9.8912
		R^2	0.8803
WMIPD	$q_t = k_{\text{diff}} t^{1/2} + C$	K_{diff}	0.1227
		C	2.5282
		R^2	0.769

the assumption that physisorption limits adsorption rate of particles onto the adsorbent, whereas in pseudo-second order model, chemisorption is considered as rate-limiting mechanism of process. The coefficient of determination (R^2) were 0.6888, 0.8803 and 0.769 for PFO, PSO and WMID models, respectively. Because of low value of R^2 and difference in experimental data and measured equilibrium sorption reflected PFO and WMID models could not define kinetics for adsorption mechanism (Table 3). It is clear that the pseudo-second order kinetic model exhibited excellent linearity with high correlation coefficient ($R^2 = 0.8803$) as compared to PFO and WMID kinetic models. Pseudo second order kinetic model had a larger correlation coefficient which reflected correlation with kinetic results (Fig. 5).

In comparison to other models, PSO kinetic model reflected as best fit to explain uptake process of CFSB for RhB dye [16]. Hence, PSO kinetic model was observed as suitable model during RhB dye uptake by coconut fruit shell biochar. Findings of present investigation reported that adsorption process was chemisorption [35].

3.3.10 Adsorption isotherm

Adsorption isotherm is applied to reflect adsorbate molecules state and their diffusion across solid and liquid phases [82]. The isotherm results are utilized for determination of optimal CFSB amount and molecular proportion of RhB dye that should be disseminated in equilibrium between solid and liquid phases. Three different isotherm models like Langmuir (LIM), Freundlich (FIM) and Temkin (TIM) were used for analyses of adsorption equilibrium data. Results revealed that RhB dye was rapidly adsorbed by CFSB at low concentration, and slowly attained to saturated sorption capacity. Experimental results were fitted by LIM, FIM and TIM models and calculated variables are

mentioned in Table 4. Langmuir isotherm explains surface with homogeneous active sites and sorption takes place onto a uniform site. Langmuir isotherm model's correlation coefficient value was high as compared to Freundlich or Temkin isotherm model. Findings reflected that LIM better described sorption mechanism, suggested that equilibrium adsorption process of RhB dye by CFSB was more inclined towards monolayer sorption where all the binding sites are similar and each active site can carry single dye molecule. Langmuir isotherm model reflected high sorption capacity (q_m) and it was 8 mg/g [83]. In addition, Langmuir constant (K_L) reflected extent of interaction between RhB dye and surface of CFSB but less value 0.0015 L/mg showed weak interaction [84].

Mei et al. [85] reported that monolayer adsorption may involve both chemical and physical sorption. Freundlich isotherm deals with multilayer sorption on a heterogeneous surface and uptake was increased exponentially with enhancement in dye concentration [67]. It focused on integrating the function of biochar and dye surface interactions. According to Freundlich isotherm model, $n < 1$ reflects sorption is chemical phenomenon, $n = 1$ sorption is linear, $n > 1$ sorption is physical [83]. In present study, $n = 1.6287$ and $1/n < 1$ (reported as 0.614), hence RhB dye sorption on CFSB was favourable, confirming that adsorption was physical process and CFSB acted as good sorbent. The high K_F value indicated more sorption capacity of CFSB.

Temkin model deals with indirect effect of dye and biochar interaction on dye elimination procedure. The heat exchange takes place between RhB dye and CFSB surface in TIM. Dye molecules sorption heat in layer will reduce with time and it will assist to calculate time for RhB dye molecules in the layer to be adsorbed by biochar.

TIM parameters, equilibrium binding constant (A_T) was analyzed from curve slope, and heat coefficient of sorption (B_T) was calculated from the intercept of curve. Because of less Temkin isotherm correlation coefficient ($R^2 = 0.9373$) obtained while removing RhB dye using CFSB, TIM was not appropriate for estimation of temperature difference in sorption process (Table 4).

Langmuir isotherm indicated best fit as compared to FIM and TIM as reflected high correlation coefficient $R^2 = 0.9818$ (Fig. 6). It depicted monolayer coverage of RhB dye on CFSB. As summarized in Fig. 6, correlation coefficient are as following: LIM (0.9818) > TIM (0.9373) > FIM (0.9215).

Langmuir constant reflected values: $q_m = 8.0906 \text{ mg g}^{-1}$, $k_L = 0.001516 \text{ L mg}^{-1}$; Freundlich constants were $K_F = 1.04081$, $n = 1.6287$ and $R^2 = 0.9215$ and Temkin constants were $b_T = 5.4571 \text{ (J mole}^{-1}\text{)}$, $A_T = 1.03125 \text{ (L mole}^{-1}\text{)}$ and $R^2 = 0.9373$.

Fig. 5 (a) Pseudo first (b) Pseudo second (c) Weber-Morris intraparticle diffusion model for sorption of RhB dye on CFSB

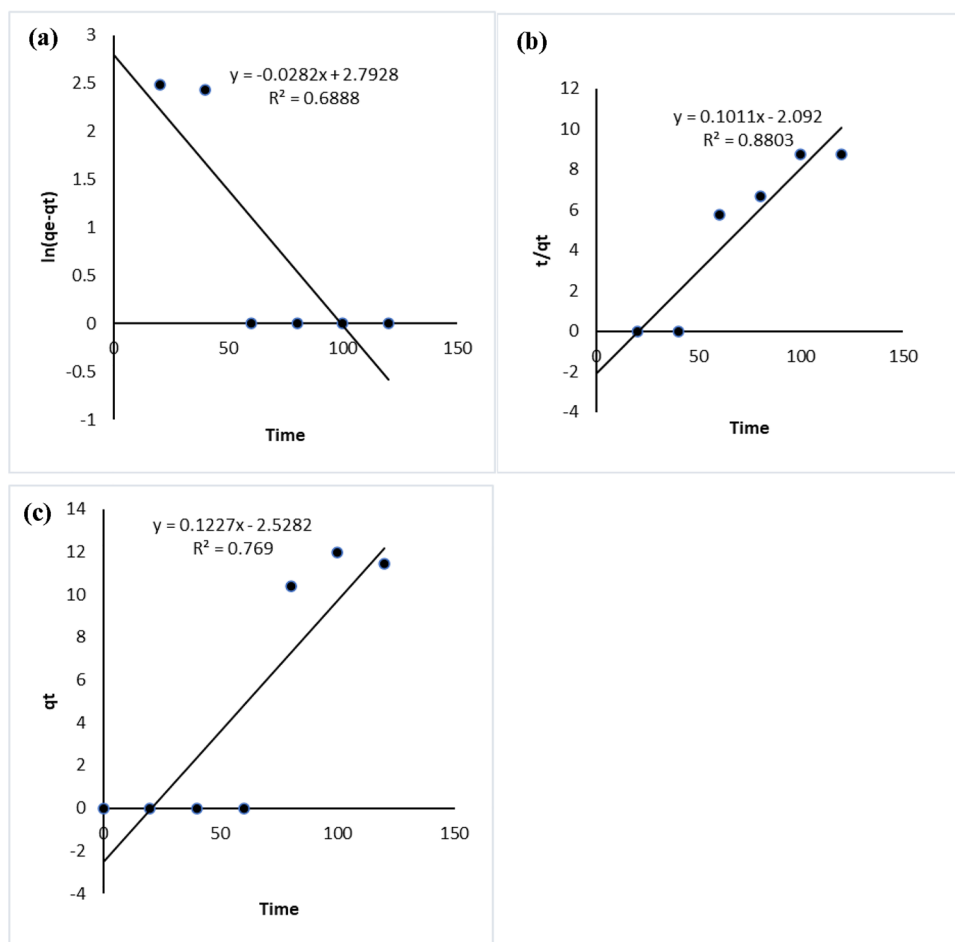


Table 4 Isotherm constant for RhB dye sorption on CFSB

Isotherm	Equation	Parameters	Value
LIM	$\frac{C_e}{q_e} = \frac{1}{q_m K_L} + \frac{C_e}{q_m}$	q_m (mg g ⁻¹) K_L (L mg ⁻¹) R^2	8.0906 0.001516 0.9818
FIM	$\ln q_e = \ln K_F + \left(\frac{1}{n}\right) \ln C_e$	n K_F (mg g ⁻¹) R^2	1.6287 1.04081 0.9215
TIM	$q_e = R_T b_T \ln(A_T) + RT/b_T \ln(C_e)$	b_T (J mole ⁻¹) A_T (L mole ⁻¹) R^2	5.4571 1.03125 0.9373

3.3.11 Thermodynamic variables

The temperature has significant effect on adsorption efficiency. Effect of sorption temperature like 30, 35, 40, 45, 50 and 55 °C on RhB dye removal was analyzed by thermodynamic parameters. Thermodynamic analysis was executed to analyse enthalpy (ΔH^0), entropy (ΔS^0), Gibbs free energy (ΔG^0). Natural log of k_d versus $1/T$ was plotted,

from which thermodynamic variables were measured and listed in Table 5.

Negative value of ΔG^0 at different temperature reflected that adsorption phenomenon was favourable and spontaneous, and in agreement with our results of kinetic as well as isotherm studies. Negative ΔH^0 value (-32.039 kJ mol⁻¹) showed exothermic nature of process and physisorption with energy exchange between system and solution. In exothermic process, heat release into solution raise temperature of the medium and impede liquid sorption onto biochar matrices [86]. It also describes decrease in sorption efficiency of RhB dye onto CFSB by increasing temperature. However, this kind of surface interaction promotes dye molecules recovery during desorption process. Positive ΔS^0 (92.802 J K⁻¹) value implied enhanced disorder and randomness at boundary of solid/liquid for RhB dye uptake. Positive value of entropy indicated that interactions between solute and solvent in aqueous solution was strong as compared to interactions between RB dye and CFSB which suggests structural modifications in dye and biochar during sorption process [87].

Fig. 6 (a) Langmuir (b) Freundlich (c) Temkin isotherm for RhB dye sorption on coconut fruit shell biochar

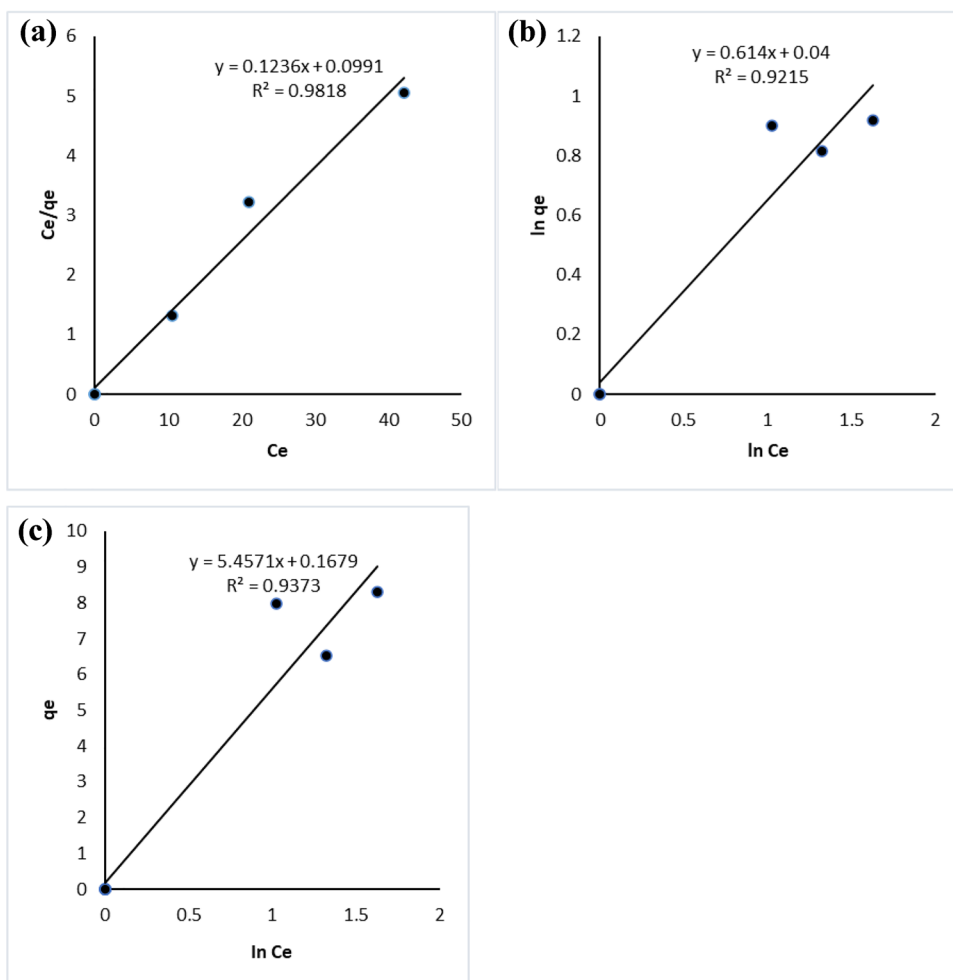


Table 5 Thermodynamic parameters for RhB dye uptake with CFSB

S.No	Temperature (°C)	ΔG^0 (kJ mol ⁻¹)	ΔH^0 (kJ mol ⁻¹)	ΔS^0 (J K ⁻¹)
1	30	-4410.947	-32.039	92.802
2	35	-3985.491		
3	40	-2796.479		
4	45	-820.541		
5	50	-1278.369		
6	55	-3182.321		

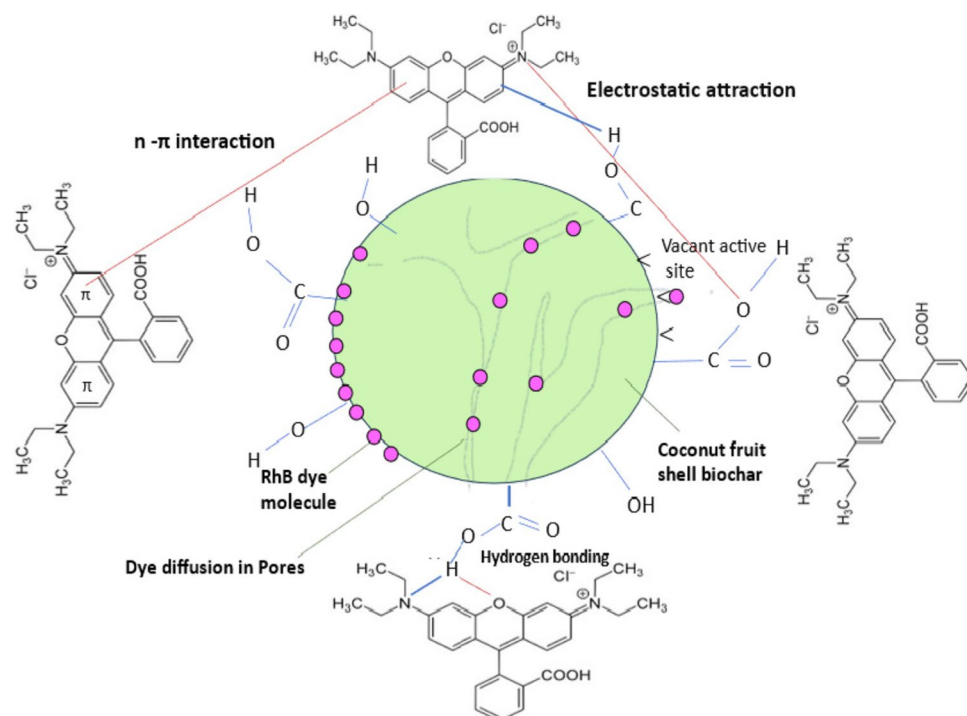
3.3.12 Adsorption mechanism

The adsorption of RhB dye on CFSB surface is regulated by various processes such as surface properties and availability of functional groups on CFSB surface, diffusion of RhB dye onto CFSB and interaction between dye and

adsorbent [88]. Three main stages are involved in adsorption process (i) transfer of RhB dye molecules from bulk solution to CFSB boundary layer via external or film diffusion, (ii) RhB dye relocation into the interior of CFSB via intra-particle diffusion, and (iii) adsorption of RhB dye into CFSB pores. In the present investigation, maximum 96% RhB dye (250 mg/L concentration) removal was reported at pH 2 by CFSB. At low pH, CFSB surface was positively charged which attracts the ionic form of RhB dye and led to increased dye adsorption.

Combining the results of both adsorption and FTIR analyses, as well as based on RhB dye structure being planar with aromatic rings, we propose that adsorption mechanism between CFSB and RhB dye molecules include pore-filling, electrostatic, n- π interaction and hydrogen bonding [89]. The proposed adsorption mechanism is presented in Fig. 7. The FTIR results show absorption band at 3405 cm⁻¹, due to the -OH group stretch, which shows presence of phenolic

Fig. 7 Adsorption mechanism between RhB dye and CFSB



compounds and alcohol groups in the CFSB. The phenolic hydroxyl groups on the surface of CFSB are expected to increase $\pi-\pi$ interactions and these dispersive interactions between aromatic rings of RhB dye and CFSB may be the primary mechanism for high adsorption capacity of CFSB for RhB dye. The stretching peaks in the range of 1505 cm^{-1} to 1511 cm^{-1} correspond to the $\pi(\text{C}=\text{C})$ bonds from different sources, including aromatic rings [90].

The acidic pH promotes hydrogen bonding of carboxyl and tertiary amine groups of RhB dye and gets protonated to oxygenated groups and reflect polar behaviour [57]. In addition to this, after RhB dye adsorption, two adsorption bands shifted to 1726 and 3407 cm^{-1} , respectively clearly indicate involvement of $\text{C}=\text{O}$ and $-\text{OH}$ groups in RhB dye adsorption, consistent with the electrical attraction between RhB dye and CFSB. The adsorption band at 2923 cm^{-1} shows presence of alkyl groups whereas band at 1732 cm^{-1} reflects carbonyl stretch, hence CFSB material is rich in carboxylic acids, ketones and esters. The FTIR spectrum reflects adsorption band at 1607 cm^{-1} , showing presence of $\text{C}=\text{C}$ linkages from various sources including aromatic rings. Additionally, intraparticle diffusion model suggests that some other mechanisms are also involved in RhB dye adsorption onto biochar. Hence, physical adsorption was carried out by Van der Waals, hydrogen bonds, $n-\pi$ interactions, polar and steric interactions whereas chemisorption involves electrons sharing between RhB dye and CFSB surface by forming a chemical bond [28]. Therefore, synergy between hydrogen bonding, $n-\pi$ interaction and pore

diffusion play an important role in adsorption of RhB dye onto CFSB.

3.3.13 Regeneration analysis

Reutilization of sorbent plays pivotal role for assessment of viability of biochar material. A good adsorbent requires renewability to obtain maximum utilization, besides high contaminants uptake efficiency. Reutilization of sorbents can decrease expenses on adsorption process, energy exhaustion for development of feasible materials and check further contamination. The alkaline and acidic reagents were used to desorb RhB dye from surface of CFSB as negative and positive functional groups were available in solution of RhB dye. Reutilized CFSB showed 88, 73, 64, 52 and 43% dye adsorption efficacy up to five cycles, respectively (Fig. 8). Reduction in RhB dye uptake efficiency was recorded after first cycle, the fast reduction in sorption efficiency may be due to blockage of adsorption sites on microspores of CFSB surface or RhB dye desorption from biochar surface. Hence, CFSB can be reutilized successfully for removal of RhB dye.

3.3.14 Phytotoxicity assessment

Impact of RhB dye was evaluated prior and after treatment of CFSB on growth and biochemical attributes of *Vigna radiata* var. Virat. Three sets were used for experimental purpose i.e. in control application of deionized water and in

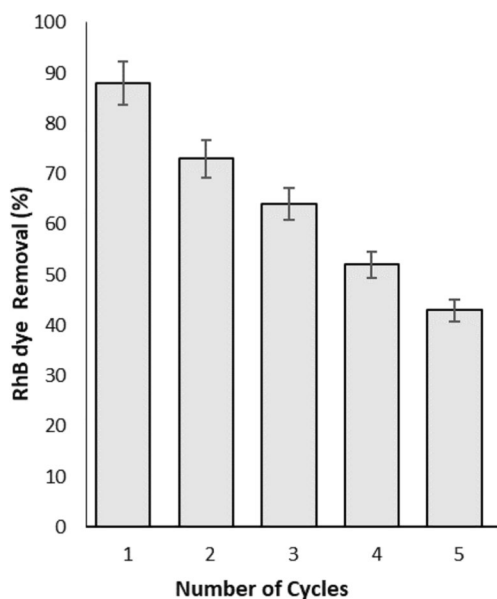


Fig. 8 Removal of Rhodamine B dye by CFSB upto five successive cycles

second and third set, solution of RhB dye (250 mg/l), CFSB treated solution of RhB dye were utilized for treatment of seeds of mung bean. Highest 97% mung bean seeds were germinated in control and only 13% germination was reported with RhB dye (250 mg/l). *Vigna radiata* demonstrated 82% germination with RhB dye solution treated with CFSB. A 4 and 10.45 cms radicle and plumule length were recorded in control which were reduced to 0.85 and 2.63 cms with treatment of RhB solution. The seedling length and vigour index of *Vigna radiata* reflected given order: Control (deionized water) > CFSB treated solution of RhB dye > RhB dye solution (Table 6). Highest biomass of *Vigna radiata* seedlings was observed in control and 68 and 77% reduction in fresh and dry weight was reported with RhB dye solution over control. Highest pigment, sugar and protein contents were recorded in *Vigna radiata* seedlings in control. Treatment of mung bean seedlings with RhB dye solution reflected 66, 72 and 77%

Table 7 Impact of RhB dye solution before and after CFSB treatment on biochemical variables of *Vigna radiata* L. variety Virat

Treatment	Total chlorophyll (mg g ⁻¹ FW)	Sugar (mg g ⁻¹ DW)	Protein (mg g ⁻¹ FW)
Control	2.57 ± 0.15 ^a	3.86 ± 0.08 ^a	23.56 ± 0.36 ^a
RhB dye solution (250 mg/l)	0.88 ± 0.02 ^c	1.09 ± 0.01 ^c	5.36 ± 0.39 ^c
CFSB treated RhB dye solution	1.45 ± 0.03 ^b	2.28 ± 0.17 ^b	16.27 ± 0.21 ^b

Values are mean ± SD of three replicates from 3 independent experiments.

Letter on data indicate significant difference among treatment at p < 0.05 significant level according to ANOVA.

decrease in chlorophyll, sugar, protein contents, respectively over control. Table 7 shows decrease in biochemical constituents of *Vigna radiata* was because of unfavourable effects of RhB dye on biochemical mechanism of plants [29, 91].

3.3.15 Coconut fruit shell biochar performance

Dye uptake capacity (q_{max}) of CFSB for RhB dye was compared with various studies conducted by earlier researchers (Table 8). Different materials showed difference in RhB dye sorption efficacy under various experimental conditions because of variation in surface area, pore size, presence of binding sites etc. Present investigation reflected that RhB dye uptake capacity of CFSB is better as compared to another sorbents, thus CFSB can be applied as sustainable alternative for RhB dye uptake.

4 Conclusion

The present investigation clearly reported that CFSB significantly eliminated RhB dye and acts as sustainable tool as compared to other available techniques. Through surface characterization of CFSB, availability of functional groups

Table 6 Impact of RhB dye solution before and after CFSB treatment on germination and growth variables of *Vigna radiata* variety Virat

Treatment	Germination (%)	Radicle length (cms)	Plumule length (cms)	Fresh weight (g)	Dry weight (g)	Vigour index
Control	97 ± 0.41 ^a	4.01 ± 0.01 ^a	10.65 ± 0.22 ^a	9.25 ± 0.22 ^a	4.23 ± 0.25 ^a	14,026.2
RhB dye solution (250 mg/l)	13 ± 0.71 ^c	0.85 ± 0.004 ^c	2.61 ± 0.28 ^c	2.93 ± 0.32 ^c	0.99 ± 0.01 ^c	452.4
CFSB treated RhB dye solution	82 ± 1.41 ^b	1.89 ± 0.02 ^b	7.24 ± 0.19 ^b	6.26 ± 0.09 ^b	2.69 ± 0.12 ^b	7699.8

Values are mean ± SD of three replicates from 3 independent experiments.

Letter on data indicate significant difference among treatment at p < 0.05 significant level according to ANOVA.

Table 8 Adsorption ability (q_{\max}) of RhB dye with different adsorbents

Sorbent material	Experimental parameters	q_{\max} (mg g ⁻¹)	References
Fly ash	pH=7.5 exposure time=80 min Dose=1 g	2.33	[92]
Kaolin	pH=9.1 exposure time=360 min Dose=2 g	7.76	[93]
Kapok pod	pH=5.45 exposure time=400 min Dose=0.1 g	33.34	[57]
Stalk corn	pH=3, exposure time=70 min, Dose=2.5 g	5.3	[68]
Walnut shell	pH=3, exposure time=30 min, Dose=0.05 g	2.29	[69]
Pomegranate peel powder	pH=5, exposure time=10 min, Dose=0.1 g	7.37	[77]
Coffee ground powder	pH=2, exposure time=3 h, Dose=50 mg	5.26	[87]
Cedar cone	pH=3; exposure time=360 min Dose=2 g	4.55	[94]
<i>Musa paradisiaca</i>	pH=4 exposure time=5 min Dose=0.1 g	6.87	[95]
Coconut fruit shell biochar	pH=2; Dose=2 g exposure time=80 min,	8.1	This study

indicate the possibility of interaction with RhB dye through hydrogen bonds, electrostatic and $n-\pi$ interactions.

RhB dye adsorption results were in best agreement with Langmuir in comparison to Freundlich and Temkin model. Kinetics for sorption reflected rate of dye uptake was best fit with pseudo second order model. Negative ΔH^0 reflected that sorption phenomenon was exothermic. CFSB significantly adsorbed RhB dye up to five successive cycles, however reduction in dye uptake onto CFSB was observed after first cycle during regeneration analysis. Therefore, CFSB can be applied as reliable sorbent for RhB dye removal from aqueous medium and reutilization of waste effluent. Compared to the untreated RhB dye effluent, CFSB treated RhB dye solution reflected good results by increasing growth and biochemical components of *Vigna radiata* seeds. But these results are far inferior when compared to the control.

Therefore, agro-waste based green adsorbents are economical, environment-friendly and affordable which may provide viable solution for removal of dye contaminants and promote waste to wealth strategy by achieving the

sustainable development goal of treating waste with waste. The findings of present investigation would lead to better understanding for development of modified biochar with enhanced sorption capacity by tailoring the functional groups for effective dye effluent decolorization for environment protection.

Acknowledgements The authors are grateful to the Researchers Supporting Project Number (RSP2024R326), King Saud University, Riyadh, Saudi Arabia.

Author contributions Conceptualization, RTK, MR, and MRS, Methodology, RTK, MR and MRS, Supervision, MR and MA; Writing-original Draft preparation, RTK, MR and MRS; Writing-Review & Editing, MR and MA; Funding acquisition MRS. All authors have read and agreed to the submitted version of the manuscript.

Data availability The data that support the findings of this study are available from the corresponding author upon reasonable request.

Declarations

Conflict of interests The authors declare no conflict of interest.

Ethical approval Not applicable.

References

- Yusuf TL, Orimolade BO, Masekela D, Mamba B, Mabuba N (2022) The application of photoelectrocatalysis in the degradation of rhodamine B in aqueous solutions: a review. *RSC Adv* 12:26176–26191. <https://doi.org/10.1039/D2RA04236C>
- Singh S, Parveen N, Gupta H (2018) Adsorptive decontamination of Rhodamine-B from water using banana peel powder: a biosorbent. *Environ Technol Innov* 12:189–195. <https://doi.org/10.1016/j.eti.2018.09.001>
- Smith CD, Jackson K, Peters H, Herrera Lima S (2020) Lack of safe drinking water for lake chapala basin communities in Mexico inhibits progress toward sustainable development goals 3 and 6. *Int J Environ Res Public Health* 17:8328. <https://doi.org/10.3390/ijerph17228328>
- Warren-Vega WM, Campos-Rodríguez A, Zárate-Guzmán AI, Romero-Cano LA (2023) A current review of water pollutants in american continent: trends and perspectives in detection, health risks, and treatment technologies. *Int J Environ Res Public Health* 20(5):4499. <https://doi.org/10.3390/ijerph20054499>
- Bentahar Y, Lomenech C, Mija A, de Jong E, Bonjour E, Jame P, Hurel C (2022) Adsorptive properties of biochar derived from biorefinery industry for basic dye removal. *Biomass Conv. Bioref.* <https://doi.org/10.1007/s13399-022-03398-w>
- Sarkar S, Echeverria-Vega A, Banerjee A, Bandopadhyay R (2021) Decolourisation and biodegradation of textile di-azo dye congo red by *Chryseobacterium geocarposphaerae* DD3. *Sustainability* 13(19):10850. <https://doi.org/10.3390/su131910850>
- Al-Buriah AK, Al-Gheethi AA, Senthil Kumar P, Radin Mohamed RMS, Yusof H, Alsharif AF, Khalifa NA (2022) Elimination of rhodamine B from textile wastewater using nanoparticle photocatalysts: a review for sustainable approaches. *Chemosphere* 287(2):132162. <https://doi.org/10.1016/j.chemosphere.2021.132162>
- Velusamy S, Roy A, Sundaram S, Kumar MT (2021) A review on heavy metal ions and containing dyes removal through graphene oxide-based adsorption strategies for textile wastewater treatment. *Chem Rec* 21(7):1570–1610. <https://doi.org/10.1002/tcr.202000153>
- Ledakowicz S, Pazdzior K (2021) Recent achievements in dyes removal focused on advanced oxidation processes integrated with biological methods. *Molecules* 26(4):870. <https://doi.org/10.3390/molecules26040870>
- Partal R, Basturk I, Hocaoglu SM, Baban A, Yilmaz E (2022) Recovery of water and reusable salt solution from reverse osmosis brine in textile industry: a case study. *Water Resour Ind* 27:100174. <https://doi.org/10.1016/j.wri.2022.100174>
- Hassan MM, Carr CM (2018) A critical review on recent advancements of the removal of reactive dyes from dyehouse effluent by ion-exchange adsorbents. *Chemosphere* 209:201–219. <https://doi.org/10.1016/j.chemosphere.2018.06.043>
- Al-Gheethi AA, Azhar QM, Kumar PS, Yusuf AA, Al-Buriah AK, Radin Mohamed RMS, Al-shaibani MM (2022) Sustainable approaches for removing Rhodamine B dye using agricultural waste adsorbents: a review. *Chemosphere* 287(2):132080. <https://doi.org/10.1016/j.chemosphere.2021.132080>
- Reck IM, Baptista ATA, Paixao RM, Bergamasco R, Vieira MF, Vieira AMS (2020) Application of magnetic coagulant based on fractionated protein of *Moringa oleifera* Lam. seeds for aqueous solutions treatment containing synthetic dyes. *Environ Sci Pollut Res* 27 (11): 12192–12201. <https://doi.org/10.1007/s11356-020-07638-2>
- Tariq M, Muhammad M, Khan J, Raziq A, Uddin MK, Niaz A, Ahmed SS, Rahim A (2020) Removal of Rhodamine B dye from aqueous solutions using photo-fenton processes and novel Ni-Cu@MWCNTs photocatalyst. *J Mol Liq* 312:113399. <https://doi.org/10.1016/j.molliq.2020.113399>
- Adegoke KA, Adegoke OR, Araoye AO, Ogunmodede J, Agboola OS, Bello OS (2022) Engineered raw, carbonaceous, and modified biomass-based adsorbents for Rhodamine B dye removal from water and wastewater. *Bioresour Technol Rep* 18:101082. <https://doi.org/10.1016/j.biteb.2022.101082>
- Ghibate R, Senhaji O, Taouil R (2021) Kinetic and thermodynamic approaches on Rhodamine B adsorption onto pomegranate peel. *Case Stud Chem Environ Eng* 3:100078. <https://doi.org/10.1016/j.cscee.2020.100078>
- Skjolding LM, LvG J, Dyhr KS, Koppl CJ, McKnight US, Bauer-Gottwein P, Mayer P, Bjerg PL, Baun A (2021) Assessing the aquatic toxicity and environmental safety of tracer compounds Rhodamine B and Rhodamine WT. *Water Res* 197:117109. <https://doi.org/10.1016/j.watres.2021.117109>
- Cheng YY, Tsai TH (2017) Pharmacokinetics and biodistribution of the illegal food colorant Rhodamine B in rats. *J Agric Food Chem* 65(5):1078–1085. <https://doi.org/10.1021/acs.jafc.6b04975>
- Sharma J, Sharma S, Bhatt U, Soni V (2022) Toxic effects of Rhodamine B on antioxidant system and photosynthesis of *Hydrilla Verticillata*. *J Hazard Mater Lett* 3:100069. <https://doi.org/10.1016/j.hazl.2022.100069>
- Sudarshan S, Bharti VS, Hari Krishnan S, Shukla SP, Rathi Bhuvaneshwari G (2022) Eco-toxicological effect of a commercial dye Rhodamine B on freshwater microalgae *Chlorella vulgaris*. *Arch Microbiol* 204(10):658. <https://doi.org/10.1007/s00203-022-03254-5>
- Kooh MRR, Dahri MK, Lim LBL (2016) Jackfruit seed as a sustainable adsorbent for the removal of Rhodamine B dye. *J Environ Biotechnol Res* 4:7–16
- Webb JM, Hansen WH, Desmond A, Fitzhugh OG (1961) Biochemical and toxicologic studies of Rhodamine B and 3,6-Diaminofluoran. *Toxicol Appl Pharmacol* 3(6):696–706. [https://doi.org/10.1016/0041-008X\(61\)90033-3](https://doi.org/10.1016/0041-008X(61)90033-3)
- Sulistina DR, Ratnawati R, Wiyasa IWA (2014) Rhodamine B increases hypothalamic cell apoptosis and disrupts hormonal balance in rats. *Asian Pac J Reprod* 3(3):180–183. [https://doi.org/10.1016/S2305-0500\(14\)60023-3](https://doi.org/10.1016/S2305-0500(14)60023-3)
- Wu J, Yan X, Li L, Gu J, Zhang T, Tian L, Su X, Lin Z (2021) High-efficiency adsorption of Cr (VI) and RhB by hierarchical porous carbon prepared from coal gangue. *Chemosphere* 275:130008. <https://doi.org/10.1016/j.chemosphere.2021.130008>
- Zhang J, Tong H, Pei W, Liu W, Shi F, Li Y, Huo Y (2021) Integrated photocatalysis-adsorption-membrane separation in rotating reactor for synergistic removal of RhB. *Chemosphere* 270:129424. <https://doi.org/10.1016/j.chemosphere.2020.129424>
- Pai S, Kini MS, Selvaraj R (2021) A review on adsorptive removal of dyes from wastewater by hydroxyapatite nanocomposites. *Environ Sci Pollut Res* 28:11835–11849. <https://doi.org/10.1007/s11356-019-07319-9>
- Koul B, Yakoob M, Shah MP (2022) Agricultural waste management strategies for environmental sustainability. *Environ Res* 206:112285. <https://doi.org/10.1016/j.envres.2021.112285>
- Bilal M, Ihsanullah I, Shah MUH, Reddy AVB, Aminabhavi TM (2022) Recent advances in the removal of dyes from wastewater using low-cost adsorbents. *J Environ Manage* 321:115981. <https://doi.org/10.1016/j.jenvman.2022.115981>
- Kapoor RT, Rafatullah M, Tajarudin HA, Siddiqui MR, Alam M (2023) Treatment of Direct Red 28 Dye through *Phoenix dactylifera* L. fruit seed biochar: equilibrium, kinetics, thermodynamics, and phytotoxicity studies. *Sustainability*. 15(21):15266. <https://doi.org/10.3390/su152115266>
- Qin C, Wang H, Yuan X, Xiong T, Zhang J, Zhang J (2020) Understanding structure-performance correlation of biochar

- materials in environmental remediation and electrochemical devices. *Chem Eng J* 382:122977. <https://doi.org/10.1016/j.cej.2019.122977>
31. Eleryan A, Yılmaz M, El-Nemr MA, Ragab S, Helal M, Has-saan MA, El Nemr A (2022) Mandarin Biochar-TETA (MBT) prepared from *Citrus reticulata* peels for adsorption of Acid Yellow 11 dye from water. *Sci Rep* 12:17797. <https://doi.org/10.1038/s41598-022-22359-x>
 32. Sathya K, Jayalakshmi H, Reddy SN, Venkataratnam M, Bandhu D (2023) Effective removal of Congo red dye using adsorbent prepared from bio-waste: isotherm, kinetic, and thermodynamic studies. *Biomass Conv Bioref*. <https://doi.org/10.1007/s13399-023-05213-6>
 33. Kim DY, Jung GB (2023) Effects of pyrolysis and ball-milling on the physicochemical and rhodamine b removal characteristics of rice-bran-derived biochar. *Appl Sci* 13:4288. <https://doi.org/10.3390/app13074288>
 34. Hou Y, Huang G, Li J, Yang Q, Huang S, Cai J (2019) Hydro-thermal conversion of bamboo shoot shell to biochar: preliminary studies of adsorption equilibrium and kinetics for rhodamine B removal. *J Anal Appl Pyrol* 143:104694. <https://doi.org/10.1016/j.jaap.2019.104694>
 35. Wang E, Huang L, Yuan X, Zhang X, Guo L, Xue C, Chen X (2021) Nutritional, phytochemical and antioxidant properties of 24 mung bean genotypes. *Food Prod Process Nutr* 3:28. <https://doi.org/10.1186/s43014-021-00073-x>
 36. Cebrian G, Condon S, Manas P (2017) Physiology of the inactivation of vegetative bacteria by thermal treatments: mode of action, influence of environmental factors and inactivation kinetics. *Foods* 6:107. <https://doi.org/10.3390/foods6120107>
 37. Giri BS, Gun S, Pandey S, Trivedi A, Kapoor RT, Singh RP, Abdeldayem OM, Rene ER, Yadav S, Chaturvedi P, Sharma N, Singh RS (2020) Reusability of brilliant green dye contaminated wastewater using corncob biochar and *Brevibacillus parabrevis*: hybrid treatment and kinetic studies. *Bioengineered* 11:743–758. <https://doi.org/10.1080/21655979.2020.1788353>
 38. Rivera-Utrilla J, Bautista-Toledo I, Ferro-García MA, Moreno-Castilla C (2001) Activated carbon surface modifications by adsorption of bacteria and their effect on aqueous lead adsorption. *J Chem Technol Biotechnol* 76:1209–1215
 39. Lagergren SK (1898) About the theory of so-called adsorption of soluble substances. *Sven Vetenskapsakad Handlingar* 24:1–39
 40. Lopez-Luna J, Ramírez-Montes LE, Martínez-Vargas S, Martínez AI, Mijangos-Ricardez OF, González-Chávez MdCA, Carrillo-González R, Solís-Domínguez FA, Cuevas-Díaz MdC, Vázquez-Hipólito V (2019) Linear and nonlinear kinetic and isotherm adsorption models for arsenic removal by manganese ferrite nanoparticles. *SN Appl Sci* 1:950. <https://doi.org/10.1007/s42452-019-0977-3>
 41. Shikuku VO, Zanella R, Kowenje CO, Donato FF, Bandeira NM, Prestes OD (2018) Single and binary adsorption of sulfonamide antibiotics onto iron-modified clay: linear and nonlinear isotherms, kinetics, thermodynamics, and mechanistic studies. *Appl Water Sci* 8:175. <https://doi.org/10.1007/s13201-018-0825-4>
 42. Ho YS, McKay G (1999) Pseudo-second order model for sorption processes. *Process Biochem* 34:451–465. [https://doi.org/10.1016/S0032-9592\(98\)00112-5](https://doi.org/10.1016/S0032-9592(98)00112-5)
 43. Weber WJ Jr, Morris JC (1963) Kinetics of adsorption on carbon from solution. *J Sanit Eng Div* 89(2):31–59. <https://doi.org/10.1061/JSEDAI.0000430>
 44. Bharathi K, Ramesh S (2013) Removal of dyes using agricultural waste as low-cost adsorbents: a review. *Appl Water Sci* 3:773–790. <https://doi.org/10.1007/s13201-013-0117-y>
 45. Ng JCY, Cheung WH, McKay G (2002) Equilibrium studies of the sorption of Cu (II) ions onto chitosan. *J Colloid Interface Sci* 255:64–74. <https://doi.org/10.1006/jcis.2002.8664>
 46. Temkin MI, Pyzhev V (1940) Kinetics of ammonia synthesis on promoted iron catalyst. *Acta Phys Chim USSR* 12:327–356
 47. Kapoor RT, Selvaraju Sivamani S (2021) Exploring the potential of *Eucalyptus citriodora* biochar against direct red 31 dye and its phytotoxicity assessment. *Biomass Convers Biorefin* 13:8011–8022. <https://doi.org/10.1007/s13399-021-01681-w>
 48. ISTA (2008) International rules for seed testing; international seed testing association, ISTA Secretariat. Bassersdorf, Switzerland
 49. Lichtenthaler HK (1987) Chlorophylls and carotenoids: pigments of photosynthetic biomembranes. *Methods Enzymol* 148:350–382. [https://doi.org/10.1016/0076-6879\(87\)48036-1](https://doi.org/10.1016/0076-6879(87)48036-1)
 50. Hedge JE, Hofreiter BT (1962) Carbohydrate chemistry 17. Whistler, R.L. and Be Miller, J. N., Eds., Academic Press, New York. 17–22
 51. Lowry OH, Rosebrough NJ, Farr AL, Randall RJ (1951) Protein measurement with the folin phenol reagent. *J Biol Chem* 193:265–275 (PMID: 14907713)
 52. Shaheen SM, Niazi NK, Hassan NEE, Bibi I, Wang H, Tsang DCW, Ok YS, Bolan N, Rinklebe J (2019) Wood-based biochar for the removal of potentially toxic elements in water and wastewater: a critical review. *Int Mater Rev* 64(4):216–247. <https://doi.org/10.1080/09506608.2018.1473096>
 53. Oliveira LMTM, Oliveira LFAM, Sonsin AF, Duarte JLS, Soletti JI, Fonseca EJS, Ribeiro LMO, Meili L (2020) Ultrafast diesel oil spill removal by fibers from silk-cotton tree: characterization and sorption potential evaluation. *J Clean Prod* 263:121448. <https://doi.org/10.1016/J.JCLEPRO.2020.121448>
 54. Tran HN, Chao HP, You SJ (2018) Activated carbons from golden shower upon different chemical activation methods: synthesis and characterizations. *Adsorpt Sci Technol* 36:95–113. <https://doi.org/10.1177/0263617416684837>
 55. Oyekanmi AA, Ahmad A, Hossain K, Rafatullah M (2019) Statistical optimization for adsorption of Rhodamine B dye from aqueous solutions. *J Mol Liq* 281:48–58. <https://doi.org/10.1016/J.MOLLIQ.2019.02.057>
 56. Gunduz G, Oral MA, Akyuz M, Aydemir D, Yaman B, Asik N, Bulbul AS, Allahverdiyev S (2016) Physical, morphological properties and raman spectroscopy of chestnut blight diseased castanea sativa mill. *Wood, cerne* 22:43–58. <https://doi.org/10.1590/01047760201622012101>
 57. Vasconcelos KC, Alencar SG, Ferro AB, Oliveira L FAM, Fonseca EJS, Bernardo VB, Zanta C LPS, Duarte J L S, Oliveira L MTM (2023) Novel kapok pods (*Ceiba pentandra* (L.) Gaerth) adsorbent and its reusability by transformation on hydrochar with an outstanding adsorptive capacity for Rhodamine B removal. *Sep Purif Technol* 326: 124787. <https://doi.org/10.1016/j.seppur.2023.124787>
 58. Matias CA, de Oliveira LJGG, Geremias R, Stolberg J, Matias CA, de Oliveira LJGG, Geremias R, Stolberg J (2020) Biosorption of rhodamine b from aqueous solution using araucaria angustifolia sterile bracts. *Rev Int Contam Ambient* 36: 97–104. <https://doi.org/10.20937/RICA.2020.36.53282>
 59. Song M, Jin B, Xiao R, Yang L, Wu Y, Zhong Z, Huang Y (2013) The comparison of two activation techniques to prepare activated carbon from corn cob. *Biomass Bioenerg* 48:250–256. <https://doi.org/10.1016/j.biombioe.2012.11.007>
 60. Yin M, Pan Y, Pan C (2019) Adsorption properties of graphite oxide for Rhodamine B. *Micro Nano Lett* 14:1211–1212. https://doi.org/10.1049/mnl.2018.5820open_in_newISSN1750-0443
 61. Lopez-Sanchez P, Martinez-Sanz M, Bonilla MR, Wang D, Gilbert EP, Stokes JR, Gidley MJ (2017) Cellulose-pectin composite hydrogels: intermolecular interactions and material properties

- depend on order of assembly. *Carbohydr Polym* 162:71–81. <https://doi.org/10.1016/j.carbpol.2017.01.049>
62. Wisniewska M, Chibowski S, Wawrzekiewicz M, Onyszko M, Bogatyrov VCI (2022) Basic Red 46 removal from sewage by carbon and silica based composite: equilibrium, kinetic and electrokinetic studies. *Molecules* 27:1043. <https://doi.org/10.3390/molecules27031043>
 63. Kamarehie B, Jafari A, Ghaderpoori M, Amin Karami M, Mousavi K, Ghaderpoury A (2019) Catalytic ozonation process using PAC/ γ -Fe₂O₃ to alizarin red S degradation from aqueous solutions: a batch study. *Chem Eng Commun* 206(7):898–908. <https://doi.org/10.1080/00986445.2018.1537266>
 64. Daouda A, Honorine AT, Bertrand NG, Richard D, Domga (2019) Adsorption of Rhodamine B onto orange peel powder. *Am J Chem* 9:142–149. <https://doi.org/10.5923/j.chemistry.20190905.02>
 65. Hii SL, Yong SY, Wong CL (2009) Removal of Rhodamine B from aqueous solution by sorption on *Turbinaria conoides*. *J Appl Phycol* 21:625–631. <https://doi.org/10.1007/s10811-009-9448-3>
 66. Gul S, Gul H, Gul M, Khattak R, Rukh G, Khan MS, Aouissi HA (2022) Enhanced adsorption of rhodamine b on biomass of cypress/false cypress (*Chamaecyparis lawsoniana*) fruit: optimization and kinetic study. *Water* 14:2987. <https://doi.org/10.3390/w14192987>
 67. Ren Z, Chen F, Wang B, Song Z, Zhou Z, Ren D (2020) Magnetic biochar from alkali-activated rice straw for removal of rhodamine B from aqueous solution. *Environ Eng Res* 25(4):536–544. <https://doi.org/10.4491/eer.2019.232>
 68. Mousavi SA, Kamarehie B, Almasi A, Darvishmotevalli M, Salari M, Moradnia M, Azimi F, Ghaderpoori M, Neyazi Z, Karami MA (2021) Removal of Rhodamine B from aqueous solution by stalk corn activated carbon: adsorption and kinetic study. *Biomass Convers Biorefin* 9:7927–7936. <https://doi.org/10.1007/s13399-021-01628-1>
 69. Shah J, Rasul Jan M, Haq A, Khan Y (2013) Removal of rhodamine B from aqueous solutions and wastewater by walnut shells : kinetics, equilibrium and thermodynamics studies. *Front Chem Sci Eng* 7:428–436. <https://doi.org/10.1007/s11705-013-1358-x>
 70. Khan M, Siddiqui MR, Otero M, Alshareef SA, Rafatullah M (2020) Removal of rhodamine B from water using a solvent impregnated polymeric dowex 5wx8 resin: statistical optimization and batch adsorption studies. *Polymers* 12(2):500. <https://doi.org/10.3390/polym12020500>
 71. Wu J, Yang J, Huang G, Xu C, Lin B (2020) Hydrothermal carbonization synthesis of cassava slag biochar with excellent adsorption performance for Rhodamine B. *J Clean Prod* 251:119717. <https://doi.org/10.1016/j.jclepro.2019.119717>
 72. Mondal PAK, MK, (2022) Green synthesis of Fe₃O₄-onion peel biochar nanocomposites for adsorption of Cr(VI), methylene blue and congo red dye from aqueous solutions. *J Mol Liq* 349(1):118161. <https://doi.org/10.1016/j.molliq.2021.118161>
 73. Enaime G, Baçaoui A, Yaacoubi A, Lübken M (2020) Biochar for wastewater treatment-conversion technologies and applications. *Appl Sci* 10:3492. <https://doi.org/10.3390/app10103492>
 74. El Haddad M, Mamouni R, Saffaj N, Lazar S (2016) Evaluation of performance of animal bone meal as a new low cost adsorbent for the removal of a cationic dye Rhodamine B from aqueous solutions. *J Saudi Chem Soc* 20:S53–S59. <https://doi.org/10.1016/j.jscs.2012.08.005>
 75. Kaya N, Yıldız Z, Ceylan S (2018) Preparation and characterisation of biochar from hazelnut shell and its adsorption properties for methylene blue dye. *Politeknik Derg* 21:765–776. <https://doi.org/10.2339/politeknik.386963>
 76. Goswami L, Kushwaha A, Kafle SR, Kim BS (2022) Surface modification of biochar for dye removal from wastewater. *Catalysts* 12:817. <https://doi.org/10.3390/catal12080817>
 77. Saigl Z M, Ahmed A M (2021) Separation of Rhodamine B dye from aqueous media using natural pomegranate peels. *Indones J Chem* 21(1): 212–224. <https://doi.org/10.22146/ijc.58592>
 78. Neupane S, Ramesh ST, Gandhimathi R, Nidheesh PV (2015) Pineapple leaf (*Ananas comosus*) powder as a biosorbent for the removal of crystal violet from aqueous solution. *Desalination Water Treat* 54:2041–2054. <https://doi.org/10.1080/19443994.2014.903867>
 79. Ambaye TG, Vaccari M, van Hullebusch ED, Amrane A, Rtimi S (2021) Mechanisms and adsorption capacities of biochar for the removal of organic and inorganic pollutants from industrial wastewater. *Int J Environ Sci Technol* 18:3273–3294. <https://doi.org/10.1007/s13762-020-03060-w>
 80. Roy TK, Mondal NK (2017) Biosorption of congo red from aqueous solution onto burned root of *Eichhornia crassipes* biomass. *Appl Water Sci* 7:1841–1854. <https://doi.org/10.1007/s13201-015-0358-z>
 81. Hu Z, Chen H, Ji F, Yuan S (2010) Removal of Congo Red from aqueous solution by cattail root. *J Hazard Mater* 173:292–297. <https://doi.org/10.1016/j.jhazmat.2009.08.082>
 82. Fu J, Chen Z, Wang M, Liu S, Zhang J, Zhang J, Han R, Xu Q (2015) Adsorption of methylene blue by a high-efficiency adsorbent (polydopamine microspheres): kinetics, isotherm, thermodynamics and mechanism analysis. *Chem Eng J* 259:53–61. <https://doi.org/10.1016/j.cej.2014.07.101>
 83. Ozturk G, Silah H (2020) Adsorptive removal of Remazol Brilliant Blue R from water by using a macroporous polystyrene resin: isotherm and kinetic studies. *Environ Process* 7:479–492. <https://doi.org/10.1007/s40710-020-00429-4>
 84. Tolkou AK, Trikalioti S, Makrogianni O, Katsoyiannis IA, Kyzas GZ (2023) Magnesium modified activated carbons derived from coconut shells for the removal of fluoride from water. *Sustain Chem Pharm* 31:100898. <https://doi.org/10.1016/j.scp.2022.100898>
 85. Mei Y, Xu J, Zhang Y, Li B, Fan S, Xu H (2021) Effect of Fe-N modification on the properties of biochars and their adsorption behavior on tetracycline removal from aqueous solution. *Biore-sour Technol* 325:124732. <https://doi.org/10.1016/j.biortech.2021.124732>
 86. Guo S, Zou Z, Chen Y, Long X, Liu M, Li X, Tan J, Chen R (2023) Synergistic effect of hydrogen bonding and π - π interaction for enhanced adsorption of rhodamine B from water using corn straw biochar. *Environ Pollut* 320:121060. <https://doi.org/10.1016/j.envpol.2023.121060>
 87. Shen K, Gondal MA (2017) Removal of hazardous rhodamine dye from water by adsorption onto exhausted coffee ground. *J Saudi Chem Soc* 21:S120–S127. <https://doi.org/10.1016/j.jscs.2013.11.005>
 88. Zare EN, Motahari A, Sillanpaa M (2018) Nanoadsorbents based on conducting polymer nanocomposites with main focus on polyaniline and its derivatives for removal of heavy metal ions/dyes: a review. *Environ Res* 162:173–195. <https://doi.org/10.1016/j.envres.2017.12.025>
 89. Cheng N, Wang B, Wu P, Lee X, XingY CM, Gao B (2021) Adsorption of emerging contaminants from water and wastewater by modified biochar: a review. *Environ Pollut* 273:116448. <https://doi.org/10.1016/j.envpol.2021.116448>
 90. Du XC, Zhu JH, Quan ZJ, Wang XC (2021) Adsorption of rhodamine B by organic porous materials rich in nitrogen, oxygen, and sulfur heteroatoms. *New J Chem* 45:3448–3453. <https://doi.org/10.1039/D0NJ05750A>
 91. Jha P, Modi N, Jobby R, Desai N (2015) Differential expression of antioxidant enzymes during degradation of azo dye reactive black 8 in hairy roots of *Physalis minima* L. *Int J Phytoremediation* 17:305–312. <https://doi.org/10.1080/15226514.2013.876963>

92. Khan TA, Ali I, Singh V V, Sharma S (2009) Utilization of fly ash as low-cost adsorbent for the removal of methylene blue, malachite green and rhodamine B dyes from textile wastewater. *J Environ Prot Sci* 3: 11–22. Corpus ID: 54812329
93. He H, Chai K, Wu T, Qiu Z, Wang S, Hong J (2022) Adsorption of Rhodamine B from simulated waste water onto kaolin-bentonite composites. *Materials* 15:4058. <https://doi.org/10.3390/ma15124058>
94. Zamouche M, Hamdaoui O (2012) Sorption of rhodamine B by cedar cone : effect of pH and ionic strength. *Energy Procedia* 18:1228–1239. <https://doi.org/10.1016/j.egypro.2012.05.138>
95. Adekola FA, Ayodele SB, Inyinbor AA (2019) Efficient Rhodamine B removal using acid and alkaline-activated *Musa paradisiaca* biochar. *Pol J Environ Stud* 28 (5): 3063–3070. <https://doi.org/10.15244/pjoes/94386>

Publisher's Note Springer Nature remains neutral with regard to jurisdictional claims in published maps and institutional affiliations.

Springer Nature or its licensor (e.g. a society or other partner) holds exclusive rights to this article under a publishing agreement with the author(s) or other rightsholder(s); author self-archiving of the accepted manuscript version of this article is solely governed by the terms of such publishing agreement and applicable law.